

Contents lists available at [SciVerse ScienceDirect](http://SciVerse ScienceDirect)

Physics Letters A

[www.elsevier.com/locate/pla](http://www.elsevier.com/locate/pla)

# Induction-detection electron spin resonance with sensitivity of 1000 spins: En route to scalable quantum computations

Aharon Blank\*, Ekaterina Dikarov, Roman Shklyar, Ygal Twig

Schulich Faculty of Chemistry, Technion – Israel Institute of Technology, Haifa, 32000 Israel

## ARTICLE INFO

### Article history:

Received 4 April 2013

Received in revised form 10 May 2013

Accepted 11 May 2013

Available online xxxx

Communicated by V.M. Agranovich

## ABSTRACT

The detection and imaging with high spatial resolution of a small number of electron spins is an important problem in science and technology. Here we show that, by making use of the smallest electron spin resonance resonator constructed to date ( $\sim 5 \mu\text{m}$ ) together with a unique cryogenic amplification scheme and submicron imaging capabilities, a sensitivity of less than 1000 electron spins is obtained with spatial resolution of  $\sim 500 \text{ nm}$ . This is the most sensitive induction-detection experiment carried out to date and it opens the door to many potential applications, one of which is the demonstration of a scalable quantum computation capability.

© 2013 Elsevier B.V. All rights reserved.

## 1. Introduction

Aside from their charge, electrons also carry the magnetic property of spin. Electrons usually team up in pairs with opposite spins, resulting in zero net spin. However, in many cases, such as free radical molecules, crystal defects, impurities, conduction/mobile electrons, and paramagnetic metal ions, electrons are not paired and their spin properties can be measured. The only general methodology for directly addressing electrons through their spin properties is ESR spectroscopy. The conventional manner of detecting unpaired electron spins is by induction detection ESR, which makes use of Faraday's law by means of a pick-up coil or a microwave (MW) resonator. Induction detection is the basic principle underlying all commercial state-of-the-art ESR systems: it permits the acquisition of high-resolution spectroscopic data with complex pulse sequences; it facilitates the use of efficient imaging methodologies (meaning that signals are acquired and averaged in *parallel* from the entire sample); and it features convenient sample handling. However, a significant drawback of conventional ESR is its relatively low sensitivity. For example, in the favorable case of a sample having a narrow ESR spectrum, commercial ESR systems require at least  $10^9$  spins to achieve a measurable signal during 1 s of acquisition [1]. Using our own highly specialized home-made system, we recently obtained a “world record” in sensitivity of  $\sim 10^6$  spins per 1 s of acquisition (often denoted as spins/ $\sqrt{\text{Hz}}$ ), which means slightly more than  $10^4$  spins in  $\sim 1 \text{ h}$  of acquisition [2]. This is still far from the ultimate limit of a single electron spin,

meaning that there is plenty of room for potential improvements. Limited sensitivity also restricts the available imaging resolution of heterogeneous samples: as the voxel size decreases, it contains fewer and fewer spins and thus quickly comes up against the sensitivity limitation barrier. Thus, commercial systems, e.g., made by Bruker, present a resolution of  $\sim 25 \mu\text{m}$ , while the systems in our laboratory recently achieved a resolution of 440 nm – limited by spin sensitivity (setting a “world record” in this field as well) [3].

There is a strong incentive to achieve ESR sensitivity capable of detecting just a few spins, accompanied by an increase in spatial resolution to the  $\sim 1\text{--}10 \text{ nm}$  range. Such an achievement will open the door to many new applications currently beyond the reach of experimental science. For example, imaging of defects, impurities, and dopants in small heterogeneous semiconductor structures [4]; measuring small numbers of spin-labeled macromolecules used for *in-cellular* structural biology studies [5]; exploring miniature spintronic systems [6]; and supporting electron spin-based quantum computing devices [7]. In view of the apparent insensitivity of induction detection, many research groups have looked into alternative detection methods in an attempt to increase sensitivity and resolution. One of the best known alternative approaches is Magnetic Resonance Force Microscopy [8], which detects the force inflicted by the spins on a sharp magnetic tip and has demonstrated a single-electron-spin detection capability and 2D imaging with nanoscale resolution [9]. Another method is Scanning Tunneling Microscopy ESR (STM-ESR) [10], which combines the high spatial resolution of STM with the electronic spin sensitivity of ESR and can measure the signal from a single spin with subnanometer 2D resolution. Other methods of possible relevance are spin-polarized STM [11], electrically-detected magnetic resonance [12],

\* Corresponding author. Tel.: +972 4 829 3679; fax: +972 4 829 5948.  
E-mail address: [ab359@tx.technion.ac.il](mailto:ab359@tx.technion.ac.il) (A. Blank).

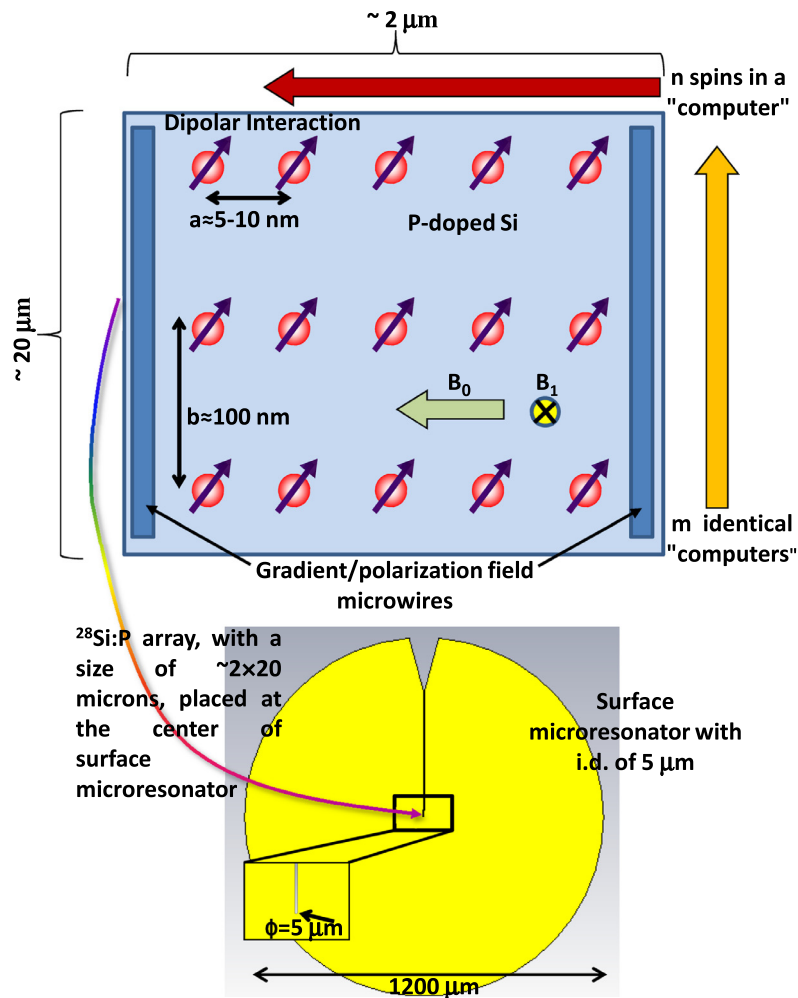


**Fig. 1.** The suggested QC scheme to be used in conjunction with ultra-high sensitivity/high-resolution induction detection [14]. A two-dimensional array of phosphorus atoms is produced inside a pure  $^{28}\text{Si}$  single crystal. The crystal is placed upside down on the center of our ultra-sensitive surface resonator [2,24,25], and operated at cryogenic temperatures. Each phosphorus nucleus in the crystal serves as a logical quantum bit (qubit), while its adjacent electron is the working qubit. The array has two lattice constants: a short one, denoted by " $a \approx 5\text{--}10\text{ nm}$ " that enables electron spins to interact through dipolar couplings along this linear vector (similar to the manner described in Ref. [16]), and a long one, denoted by " $b \approx 100\text{ nm}$ " that separates many identical copies of the same individual vector computers. Individual spins can be addressed by applying a large magnetic field gradient with DC current into microwires (separating the spins in the frequency domain), and the state of all spins can be read out in parallel via a one-dimensional image along the crystal's  $x$ -axis. All parallel identical computer vectors should give the same vector of spin states, thereby increasing the measured signal and also greatly minimizing the need for quantum error correction due to random spin flips, since the measured result averages over  $\sim 100\text{--}1000$  spins per qubit. Information can be swapped between working electron spins and logical nuclear spins through combined radiofrequency (RF) and microwave (MW) pulse sequences, as described in Ref. [26].

and indirect spin detection via diamond nitrogen-vacancy (NV) centers [13]. However, while these and other new techniques are very impressive, they all have inherent limitations that result in restricted applicability. They (a) are highly specific to particular samples and experimental conditions, (b) require complex procedures for sample preparation, (c) lack advanced spectroscopic capabilities, (d) operate efficiently only on or very close to the surface (a few nanometers), and (e) use mechanical movements to scan and image samples in a sequential manner. Thus, in many ways, they can be considered only as complementary to induction detection schemes and are not capable of providing answers to most of the scientific and technological challenges that involve a small number of spins and heterogeneous samples.

Here we push the barriers of induction detection ESR capabilities significantly further and demonstrate sensitivity of less than 1000 spins accompanied by submicron spatial resolution. The importance of this development goes well beyond a mere linear improvement in sensitivity since this level of spin sensitivity opens the door for the first time to the implementation of a unique scheme of scalable spin-based quantum computation (QC) [14].

## 2. High sensitivity/high resolution induction detection ESR for QC

Spin-based quantum computation in the solid state is considered to be one of the most promising approaches to scalable quantum computers [7,15–17]. However, it faces problems such as initializing the spins, selectively addressing and manipulating single spins, and reading out the state of the individual spins. In order to realize a scalable quantum computer it is necessary to comply with the so-called "DiVincenzo criteria" [18], which include: (i) having a scalable physical system with well-characterized qubits; (ii) the ability to initialize the state of the qubits to a simple fiducial state such as  $|000\dots\rangle$ ; (iii) long coherence times, much longer than the gate operation time; (iv) a universal set of quantum gates; and (v) a qubit-specific measurement capability. We have recently sketched a scheme that potentially solves all of these problems, as shown in Fig. 1 [14]. It is based on the use of a uniquely fabricated  $^{28}\text{Si:P}$  array, coupled with high static magnetic field gradients and fast switchable high polarizing fields, along with ultra-sensitive induction-detection ESR. The use of the electron and nuclear spins in  $^{28}\text{Si:P}$  as qubits is known to be very promising in the context of

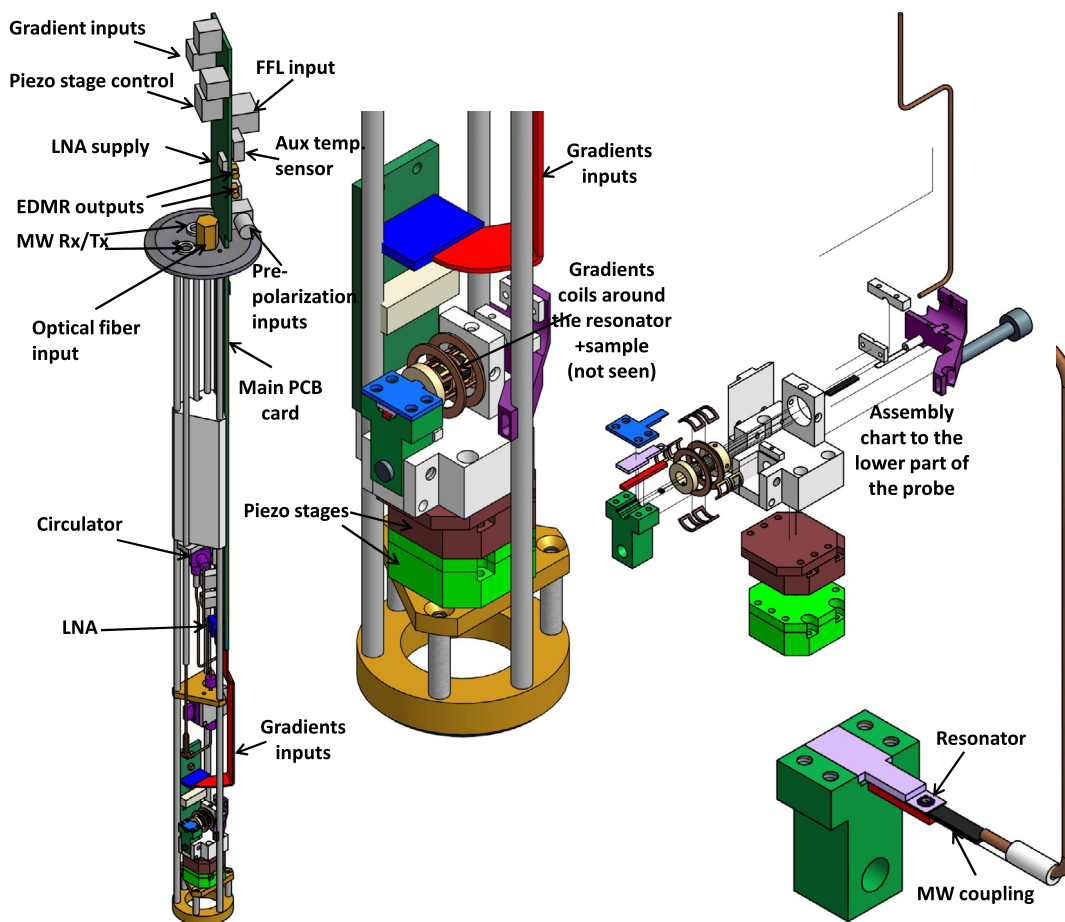


**Fig. 2.** The new cryogenic probe that was employed in the experiments. The resonator is operated in reflection mode. Both the cryogenic magnetically-shielded circulator (model PTG1218KCSZ from QuinStar Technology Inc., USA), and the first low-noise amplifier (model LNF-LNC6\_20A from Low Noise Factory AB, Sweden) are cooled to cryogenic temperatures. The probe has several functionalities: (a) It facilitates the use of optical excitation by optical fiber, if needed. (b) It enables the generation of static and pulsed magnetic field gradients and polarization fields in all 3 axes. (c) It supports the use of current sensors for potential experiments of electrically-detected magnetic resonance (EDMR). (d) It has 2 (and in other designs, 3) independent piezo stages to control the coupling of the microwave line to the resonator. (e) It makes provisions for independent temperature sensor readings. A specially-designed 10-layer main PCB (printed circuit board) supports the connectivity of all these inputs/outputs and is also used for the field frequency lock (FFL) module [3] that maintains the “on-resonance” condition even when the main static field drifts slowly.

QCs [19]. The long coherence time of this system’s electrons and nuclei (in the range of seconds [20]) compared to the short interaction and manipulation times of the electron spins (in the range of 10–1000 ns), puts it on a par with the most advanced ideas for QCs. In addition, the electrons’ spin-lattice relaxation time in  $^{28}\text{Si:P}$  can be effectively controlled by means of light, making it possible to greatly increase spin polarization using an appropriate short pulse in a large static field [14]. The fabrication of such an array is somewhat beyond the current capabilities of nanotechnology, but not by far [21]. Apart from the unique sample itself, the major missing component required for the realization of the proposed scheme is an induction-detection capability to detect the signal from only  $\sim 100$ –1000 electron spins (in a reasonable averaging time of maximum a few hours). Thus, while single-spin sensitivity is not required to operate such QCs, these sensitivity values are still a great challenge and thus seem to make the proposed scheme unattainable.

### 3. The sensitivity of induction detection ESR

The absolute spin sensitivity in induction detection ESR is proportional to  $1/\sqrt{V_c}$ , where  $V_c$  is the effective volume of the resonator employed [3]. Commercial systems commonly employ relatively large resonators which, at a typical frequency of  $\sim 10$  GHz, have an effective volume ranging from a few milliliters down to a

few microliters at most. Recently, extensive work has been carried out with the aim of designing and constructing resonators with much smaller effective volumes while maintaining reasonably high quality ( $Q$ ) factors [3,22,23]. The latest of these efforts is our continued work on a set of so-called surface loop-gap microresonators that have a very small internal diameter, reaching just  $5\ \mu\text{m}$  ( $V_c \approx 0.1\ \text{nl}$  – see Fig. 1) in our most recent designs, for operation at the Ku microwave band ( $\sim 15$ –17 GHz) [24]. This resonator exhibited a measured spin sensitivity of  $\sim 3 \times 10^7$  spins/ $\sqrt{\text{Hz}}$  (or  $\sim 5 \times 10^5$  spins for 1 hour of averaging) at 15.76 GHz for a sample of  $\gamma$ -irradiated  $\text{SiO}_2$ , measured at room temperature [24]. In parallel, we have also recently measured a sample of  $^{28}\text{Si:P}$  at a temperature of 10 K using a slightly larger resonator featuring a  $20\ \mu\text{m}$  internal diameter, which provided spin sensitivity of  $\sim 4000$  spins (with signal-to-noise-ratio (SNR) of 1) for 2 h of acquisition time [25].

### 4. Experimental

Our home-made pulsed ESR imaging system is described in Ref. [3]. The measurements described here were also carried out with a  $10\ \mu\text{m}$ -thick  $^{28}\text{Si:P}$  sample containing  $10^{16}$  P atoms in  $1\ \text{cm}^3$  (described in Ref. [2]) at a temperature of 9.5 K using the  $20\ \mu\text{m}$  and the  $5\ \mu\text{m}$  resonators, which are the smallest of their kind. The use of such small resonators at cryogenic temper-

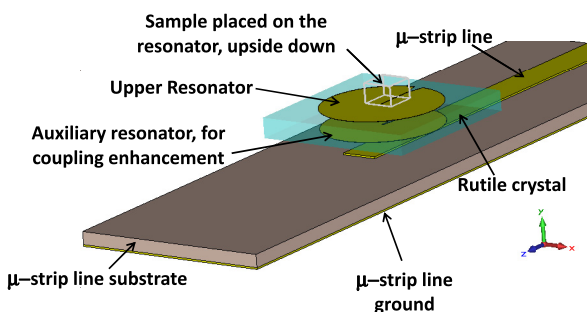


**Fig. 3.** Details of the microwave coupling configuration and the position of the sample with respect to the resonator. The image shows the 5  $\mu\text{m}$  resonator, which uses a 20  $\mu\text{m}$  resonator on the bottom part as an auxiliary resonator to facilitate efficient microwave energy coupling (see Ref. [24]).

atures enabled us to improve on the sensitivity obtained from our previous measurements. Furthermore, additional significant improvements in spin sensitivity for both resonators were obtained through the use of a newly fabricated cryogenic probe (Fig. 2) that incorporates a cryogenic low-noise amplifier (LNA) and a cryogenic magnetically-shielded circulator. In the new microwave configuration, the pulsed microwave excitation signal goes first through the circulator, then reaches the resonator and returns to the circulator and to the cryogenic amplifier. Since both the circulator and the amplifier are cooled to  $\sim 10$  K, the noise in the detection system is decreased by a factor of  $\sim 5$  compared to the use of an external circulator and amplifier. It should be noted that such cryogenic low-noise amplifiers are very sensitive to the applied microwave power and a level of more than  $\sim 1$  mW would damage them. Nevertheless, we can handle this limitation without requiring a protection switch before the cryogenic amplifier (which would greatly deteriorate its noise performance) because we employ a surface resonator for which a power level of  $\sim 0.5$  mW is more than enough to efficiently excite the spins in the sample in pulsed ESR [24]. The probe itself has also microimaging capabilities (Fig. 2) and is a greatly improved version of the one described in Ref. [25]. During the experiment the sample, which is  $\sim 1.5 \times 1.5$  mm in size, is placed face down on the resonator (Fig. 3).

**5. Results and discussion**

The results of our experiments with the  $^{28}\text{Si:P}$  sample are shown in Figs. 4–5. For signal acquisition, we employed a Carr–Purcell–Meiboom–Gill (CPMG) pulse sequence with a repetition rate of 1000 Hz,  $\pi/2$ – $\pi$  pulse separation,  $\tau = 1.2$   $\mu\text{s}$ , and a data acquisition window of 1  $\mu\text{s}$ . Fig. 4 shows the acquired echo signal compared to the noise level for an averaging time of 1 s, i.e., for 1000 CPMG trains (data was also averaged along each 160- $\pi$ -pulse CPMG train). The measured SNR was  $\sim 1486$  ( $\sim 581$ ) for the 20- $\mu\text{m}$  (5- $\mu\text{m}$ ) resonator, when tuned to its resonance frequency of 14.62 (15.18) GHz, at 9.5 K. The full-width-half-maximum line width was measured to be 0.85 (Fig. 4 left) and 0.38 G (Fig. 4 right), and is dominated by static field inhomogeneity, which was found to vary from resonator to resonator (due to differences in metallic parts that are slightly magnetic). The number of spins in the effective volume of these two resonators can be estimated to be not more than  $\sim 4.8 \times 10^7$  ( $\sim 2.25 \times 10^7$ ), based on the calculated volume of the resonator from which most of the signal is acquired,  $\sim 60 \times 20 \times 4$  ( $5 \times 150 \times 3$ ) [ $\mu\text{m}^3$ ] [24]. This provides an initial estimate of spin sensitivity (for SNR = 1) of  $\sim 3.2 \times 10^4$  ( $\sim 3.87 \times 10^4$ ) spins/ $\sqrt{\text{Hz}}$  for the 20- $\mu\text{m}$  (5- $\mu\text{m}$ ) resonator employed here.

At first glance it seems that the use of the smaller resonator did not increase spin sensitivity, and even reduced it, while in theory it should have improved the latter by a factor of  $\sim 1.62$  compared to the larger resonator [24]. However, our calculations, based on the echo signal, assumed constant ESR sensitivity throughout the resonator’s effective volume, while in practice some parts of the resonators are more sensitive than others (and these are the sections in which it would be preferable to place small samples) [24]. Thus, in order to provide a solution to this issue and, mainly, to offer more exact measured values for the spin sensitivity of our resonators *at their most sensitive spot*, we acquired two-dimensional high resolution images of the sample in the resonators, as shown in Fig. 5. These imaging results also demonstrate our ability to obtain a very high spatial resolution with this type of sample – which is of relevance for our proposed QC scheme. When looking at Fig. 5 it should be mentioned that, although the sample is positioned so that it covers the resonator’s entire central area (Fig. 2), the signal originates only from areas where the resonator has a strong

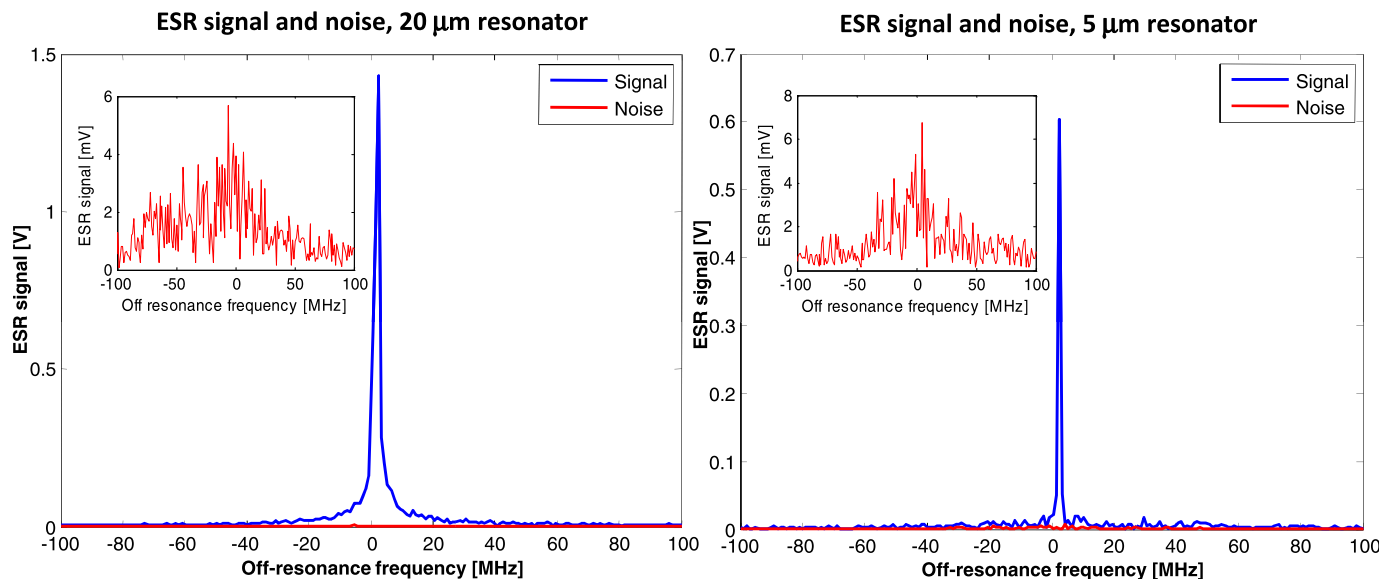


**Fig. 4.** ESR signal (blue lines) compared to noise level (red lines, obtained at 100-G off-resonance with 1-s averaging time) for the  $^{28}\text{Si:P}$  sample placed on the 20- $\mu\text{m}$  (left) and 5- $\mu\text{m}$  (right) resonators. The two inserts show the noise level in millivolts measured at 50- $\Omega$  impedance (blown up by a factor of 1000), to enable comparison to the signal in volts. (For interpretation of the references to color in this figure legend, the reader is referred to the web version of this Letter.)

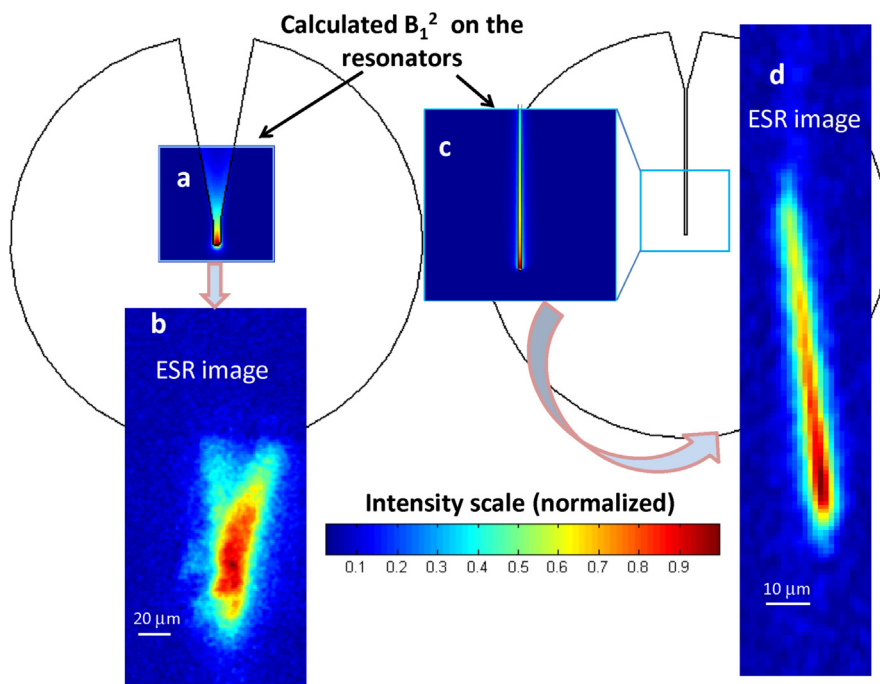


**Fig. 5.** Calculated and measured microwave magnetic field distribution ( $B_1^2$ ) close to the resonator's surface. (a) Calculated  $B_1^2$  on the 20- $\mu\text{m}$  resonator, summed over the first 5  $\mu\text{m}$  above the surface. (b) Two-dimensional ESR image taken with a flat  $^{28}\text{Si:P}$  sample placed on the resonator. (c) The same as in (a) but for the 5- $\mu\text{m}$  resonator, summed over the first 3  $\mu\text{m}$  above the surface (the area at the center of the resonator is blown up for better clarity). (d) The same as in (b) but for the 5- $\mu\text{m}$  resonator.

microwave magnetic field component ( $B_1$ ) and the image should correspond to the calculated spatial distribution of  $B_1^2$  [23]. Image resolution was limited by the SNR and not by our pulsed field gradients' capabilities (which can support resolution of even 80 nm, if SNR is not a limitation [3]). That is to say, for each resonator we chose the best possible 2D resolution for which the image's SNR would still be reasonable (for overnight acquisition). Thus, for the 20- $\mu\text{m}$  (5- $\mu\text{m}$ ) resonator the size of each voxel in this image is  $0.5 \times 0.75$  ( $1 \times 1.2$ )  $\mu\text{m}$  and, although the sample's thickness is 10  $\mu\text{m}$ , most of the signal originates only in the first 5 (3)  $\mu\text{m}$  above the resonator's surface, due to the fast decay of  $B_1$  when going out of plane [24,25]. Thus, the 2D imaging experiment, combined with the calculated data for the out-of-plane field, provides us with a voxel volume of 1.87 (3.6)  $\mu\text{m}^3$  which contains  $1.87 \times 10^4$  ( $3.6 \times 10^4$ ) spins for the 20- $\mu\text{m}$  (5- $\mu\text{m}$ ) resonator. The voxel with the maximum signal-to-noise ratio (where the noise is measured at the image's peripheral parts) is found to be with SNR of 78 (97), giving a spin sensitivity (with SNR = 1) of 240 (370) spins for the total measurement time employed for image acquisition (10 hours for both images). In other words, based on the ESR imaging results, spin sensitivity is found to be  $240 \times \sqrt{(3600 \times 10)} \approx 4.5 \times 10^4$  ( $370 \times \sqrt{(3600 \times 10)} \approx 7.0 \times 10^4$ ) spins/ $\sqrt{\text{Hz}}$  for the 20- $\mu\text{m}$  (5- $\mu\text{m}$ ) resonator employed here, which is slightly worse than our above estimate formulated on the bases of the 1-s-echo data acquisition (Fig. 4). It should be noted, however, that the limited stability of our system may explain the reduction in performance during the prolonged imaging data acquisition period (used for averaging).

The sensitivity obtained through the present measurements corresponds well to the theoretical predictions of spin sensitivity of  $\sim 8.6 \times 10^4$  ( $\sim 5.3 \times 10^4$ ) spins/ $\sqrt{\text{Hz}}$  for the 20- $\mu\text{m}$  (5- $\mu\text{m}$ ) resonator employing this type of sample [24]. Although the 5- $\mu\text{m}$  resonator generated lower experimental sensitivity than the 20- $\mu\text{m}$  resonator and is further apart from the theoretical prediction, we believe that this is due to our limited sample-resonator attachment capability. This means that something, probably a small amount of dust, prevented us from placing the sample right on top of

the resonator, and this has a greater effect on the signal in the 5- $\mu\text{m}$  resonator than in the larger one. Thus, it is highly plausible that the theoretical values do represent effective measurements achievable with a more direct sample/resonator coupling, where the 5- $\mu\text{m}$  resonator would be the most sensitive one.

Another point of importance is the heterogeneous signal amplitude apparent in the ESR images, which originates from the heterogeneity of the resonators' microwave  $B_1$  component. Clearly, such heterogeneity must be thoroughly mapped, either by calculation or by means of an experiment (as the one presented here), employing homogeneous samples. Such a-priori mapping can then be further used to provide accurate quantitative spin concentration results for a heterogeneous sample of interest that fits inside the active volume of the resonators.

## 6. Conclusions

The experimental results for spin sensitivity demonstrated here are by far the best obtained to date with induction-detection ESR and can support many important future experiments with spin-limited paramagnetic materials, as noted in the introduction, and specifically, the demonstration of a unique scalable QC scheme [14]. Finally, recent detailed analysis showed that spin sensitivity can be further improved by a factor of up to  $\sim 25$  through the use of higher static fields (3.4 T) and smaller resonators (down to  $\sim 1$   $\mu\text{m}$ ) [24]. This would also enable to improve the 2D resolution further by a factor of  $\sim \sqrt{25} = 5$ , given that it is currently limited by the SNR and not by the strength of our gradient pulses.

## Acknowledgements

This work was partially supported by grant #213/09 from the ISF, grant #201665 from the ERC, grant #G-1032-18.14/2009 from the GIF, and by RBNI and MNFU at the Technion. We greatly acknowledge Dr. Wayne D. Hutchison (University of New South Wales, Australia) for supplying us with the  $^{28}\text{Si:P}$  sample.

**References**

- [1] D. Schmalbein, G.G. Maresch, A. Kamlowski, P. Hofer, *Appl. Magn. Reson.* 16 (1999) 185.
- [2] Y. Twig, E. Dikarov, W.D. Hutchison, A. Blank, *Rev. Sci. Instrum.* 82 (2011) 076105.
- [3] L. Shtirberg, Y. Twig, E. Dikarov, R. Halevy, M. Levit, A. Blank, *Rev. Sci. Instrum.* 82 (2011) 043708.
- [4] G.D. Watkins, *Phys. Solid State* 41 (1999) 746.
- [5] T.F. Prisner, I. Krstic, R. Hansel, O. Romainczyk, J.W. Engels, V. Dotsch, *Angew. Chem., Int. Ed. Engl.* 50 (2011) 5070.
- [6] D.D. Awschalom, N. Samarth, *Physics* 2 (2009) 50.
- [7] V. Cerletti, W.A. Coish, O. Gywat, D. Loss, *Nanotechnology* 16 (2005) R27.
- [8] D. Rugar, R. Budakian, H.J. Mamin, B.W. Chui, *Nature* 430 (2004) 329.
- [9] C.L. Degen, M. Poggio, H.J. Mamin, C.T. Rettner, D. Rugar, *Proc. Natl. Acad. Sci. USA* 106 (2009) 1313.
- [10] C. Durkan, M.E. Welland, *Appl. Phys. Lett.* 80 (2002) 458.
- [11] F. Meier, L.H. Zhou, J. Wiebe, R. Wiesendanger, *Science* 320 (2008) 82.
- [12] W. Harneit, C. Boehme, S. Schaefer, K. Huebener, K. Fostiropoulos, K. Lips, *Phys. Rev. Lett.* 98 (2007) 216601.
- [13] P. Hemmer, B. Grotz, J. Beck, P. Neumann, B. Naydenov, R. Reuter, F. Reinhard, F. Jelezko, J. Wrachtrup, D. Schweinfurth, B. Sarkar, *New J. Phys.* 13 (2011) 055004.
- [14] A. Blank, *Quantum Inf. Process.* (2013), <http://dx.doi.org/10.1007/s11128-013-0577-x>, in press.
- [15] B.E. Kane, *Nature* 393 (1998) 133.
- [16] W. Harneit, C. Meyer, A. Weidinger, D. Suter, J. Twamley, *Phys. Status Solidi B* 233 (2002) 453.
- [17] C.Y. Ju, D. Suter, J.F. Du, *Phys. Lett. A* 375 (2011) 1441.
- [18] D.P. DiVincenzo, *Fortschr. Phys.* 48 (2000) 771.
- [19] J.J.L. Morton, D.R. McCamey, M.A. Eriksson, S.A. Lyon, *Nature* 479 (2011) 345.
- [20] A.M. Tyryshkin, S. Tojo, J.J.L. Morton, H. Riemann, N.V. Abrosimov, P. Becker, H.J. Pohl, T. Schenkel, M.L.W. Thewalt, K.M. Itoh, S.A. Lyon, *Nat. Mater.* 11 (2012) 143.
- [21] M.Y. Simmons, F.J. Ruess, K.E.J. Goh, W. Pok, T. Hallam, M.J. Butcher, T.C.G. Reusch, G. Scappucci, *Int. J. Nanotechnol.* 5 (2008) 352.
- [22] R. Narkowicz, D. Suter, I. Niemeyer, *Rev. Sci. Instrum.* 79 (2008) 084702.
- [23] Y. Twig, E. Suhovoy, A. Blank, *Rev. Sci. Instrum.* 81 (2010).
- [24] Y. Twig, E. Dikarov, A. Blank, *Mol. Phys.* (2013), <http://dx.doi.org/10.1080/00268976.2012.762463>, in press.
- [25] Y. Twig, E. Dikarov, A. Blank, *J. Magn. Reson.* 218 (2012) 22.
- [26] J.J.L. Morton, A.M. Tyryshkin, R.M. Brown, S. Shankar, B.W. Lovett, A. Ardavan, T. Schenkel, E.E. Haller, J.W. Ager, S.A. Lyon, *Nature* 455 (2008) 1085.